Beyond modelocking: High repetition-rate frequency combs derived from a continuous-wave laser

by

Daniel C. Cole

B.S., Washington University in St. Louis, 2012

M.S., University of Colorado, 2015

A thesis submitted to the

Faculty of the Graduate School of the

University of Colorado in partial fulfillment

of the requirements for the degree of

Doctor of Philosophy

Department of Physics

2018

This thesis entitled:
Beyond modelocking: High repetition-rate frequency combs derived from a continuous-wave laser
written by Daniel C. Cole
has been approved for the Department of Physics

Scott A. Diddams

Reader Two

Date

The final copy of this thesis has been examined by the signatories, and we find that both the content and the form meet acceptable presentation standards of scholarly work in the above mentioned discipline.

Cole, Daniel C. (Ph.D., Physics)

Beyond modelocking: High repetition-rate frequency combs derived from a continuous-wave laser

Thesis directed by Dr. Scott A. Diddams

Optical frequency combs based on modelocked lasers have revolutionized precision metrology by facilitating measurements of optical frequencies, with implications both for fundamental scientific questions and for applications such as fast, broadband spectroscopy. In this thesis, I describe advances in the generation of frequency combs without modelocking in platforms with smaller footprints and higher repetition rates, with the ultimate goal of bringing frequency combs to new applications in a chip-integrated package. I discuss two approaches for comb generation: parametric frequency conversion in Kerr microresonators and active electro-optic modulation of a continuous-wave laser. After introducing microresonator-based frequency combs (microcombs), I discuss two specific developments in microcomb technology: First, I describe a new, extremely reliable method for generation of soliton pulses through the use of a phase-modulated pump laser. This technique eliminates the dependence on initial conditions that was formerly a universal feature of these experiments, presenting a solution to a significant technical barrier to the practical application of microcombs. Second, I present observations of *soliton crystal* states with highly structured 'fingerprint' optical spectra that correspond to ordered pulse trains exhibiting crystallographic defects. These pulse trains arise through interaction of solitons with avoided mode-crossings in the resonator spectrum. I also discuss generation of Kerr soliton combs in the Fabry-Perot (FP) geometry, with a focus on the differences between the FP geometry and the ring geometry that has been the choice of most experimenters to date. Next, I discuss combs based on electro-optic modulation. I introduce the operational principle, and then describe the first self-referencing of a frequency comb of this kind and a proof-of-principle application experiment. Finally, I discuss a technique for reducing the repetition rate of a high repetition-rate frequency comb, which will be a necessary post-processing step for some applications.

Contents

Figures

Chapter 1

Theory of Kerr frequency combs in Fabry-Perot resonators

Generation of Kerr frequency combs in the ring-resonator geometry appears quite promising for applications. However, a second possibility is to use the same processes for comb generation, but with a Fabry-Perot (FP) resonator geometry. The FP geometry offers a new degree of freedom relative to the ring resonator, which is the possibility to employ chirped mirrors, mirror coatings, or distributed Bragg reflectors, and therefore exert greater control over the total cavity dispersion. Other differences with the ring geometry may ultimately prove important, for example the smaller footprint possible in a cavity of total length L with the FP geometry versus the ring geometry could allow for denser and more flexible integration of Kerr combs in photonics systems. Kerr-comb generation in an FP cavity was reported in 2009 Ref. [36] and soliton generation using a pulsed pump laser was recently described in Ref. [37].

In this chapter we present a brief theoretical investigation of the difference in the nonlinear dynamics that occur in a Kerr-nonlinear FP resonator versus a Kerr-nonlinear ring resonator. Our starting point is the Fabry-Perot Lugiato-Lefever equation (FP-LLE), which is derived in detail in Ref. [**Cole2018a**], beginning from a set of coupled equations that describe the interaction of the envelopes for the forward- and backward-propagating fields in the cavity with the Kerr medium. A derivation of equivalent coupled mode equations is provided in Ref. [37]. We do not reproduce the derivation of the equation here; our goal is to understand its description of Kerr-comb dynamics. The equation is:

$$\frac{\partial\psi}{\partial\tau} = -(1+i\alpha)\psi + i|\psi|^2\psi - i\frac{\beta_2}{2}\frac{\partial^2\psi}{\partial\theta^2} + 2i\psi\left\langle|\psi|^2\right\rangle + F. \tag{1.1}$$

Here, $< g >$ denotes the spatial average over the domain: $< g >= \frac{1}{2\pi}\int_{-\pi}^{\pi} d\theta\, g(\theta)$. This equation is identical to the LLE for the ring cavity except for the term $2i\psi\left\langle|\psi|^2\right\rangle$ describing modulation by twice the average of the intracavity power. The coordinate θ is defined as $\theta = 2\pi z/2L$, where z is a co-moving longitudinal coordinate (so that, for example, solitons are stationary functions of θ) on a domain $-L \le z \le L$; L is the physical length of the Fabry-Perot cavity. The time τ is once again normalized to twice the photon lifetime τ_γ: $\tau = t/2\tau_\gamma$. The normalized experimental parameters in the FP-LLE are the same as in the LLE for the ring cavity, with α the detuning, β_2 the dispersion, and F^2 the pump power:

$$\alpha = -\frac{2(\omega_o - \omega_c)}{\Delta\omega_o}, \tag{1.2}$$

$$\beta_2 = -\frac{2D_2}{\Delta\omega_{tot}} = -\frac{2}{\Delta\omega_o}\frac{\partial^2\omega_\mu}{\partial\mu^2}\bigg|_{\mu=0}, \tag{1.3}$$

$$F^2 = \frac{8g_o\Delta\omega_{ext}}{\Delta\omega_{tot}^3}\frac{A_{eff}}{A_{in}}\frac{n_o}{n_{ext}}\frac{P}{\hbar\omega_o}. \tag{1.4}$$

In the above, ω_μ represents the set of resonance frequencies of the cavity including the effects of dispersion, with $\mu = 0$ indexing the pumped mode (see e.g. Ref. [83]). The cavity loss and coupling rates $\Delta\omega_{tot}$ and $\Delta\omega_{ext}$ are related to the mirror reflectivity R and transmission T via $\Delta\omega_{tot} = (1-R)c/n_gL$ (where two identical mirrors are assumed) and $\Delta\omega_{ext} = cT/2n_gL$, with

$n_g = c/v_g$ the group index. The quantities A_{in} and A_{eff} represent the mode's effective area πw_{in}^2 (for a Gaussian mode of radius w) at the input mirror and the same averaged over the cavity of length L, $\frac{\pi}{L}\int dz\, w(z)^2$, respectively. Further, $g_o = n_2\hbar\omega_o^2 D_1/(2\pi n_g A_{eff})$ is the nonlinear gain parameter, where $D_1 = \frac{\partial\omega_\mu}{\partial\mu}\Big|_{\mu=0}$ is the cavity free-spectral range in angular frequency (here and in Eq. (1.3) μ is treated as a continuous variable). The nonlinear index n_2 is related to the third-order susceptibility via $\chi^{(3)} = (4/3)n_o^2\epsilon_o c n_2$, where n_o is the refractive index of the nonlinear medium. The power $P = \eta P_{inc}$ denotes the mode-matched power, with mode-matching factor η and power P_{inc} incident on the input mirror, and n_{ext} is the refractive index of the medium external to the cavity.

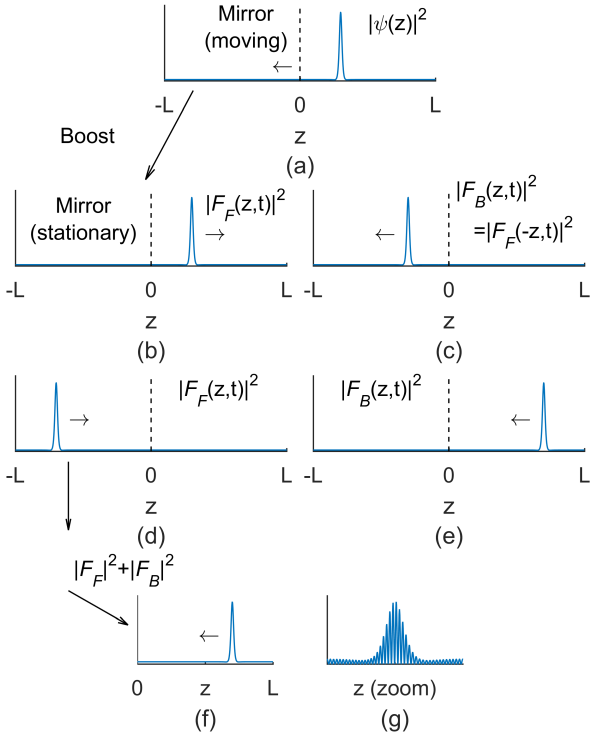

Figure 1.1: **Relationship between the physical field in the Fabry-Perot cavity and the co-moving field ψ.** (a) A soliton stationary solution to the FP-LLE in the co-moving domain of length $2L$, in which the physical components of the cavity (e.g. mirror) move. (b) Intensity of the field F_F in the lab frame, in which the cavity is stationary. (c) Intensity of F_B in the lab frame, related to F_F by reflection about the origin. (d,e) Depictions of the same after propagation for half of the cavity round-trip time. (f) Total intensity of the field on the physical domain $0 \le z \le L$. (g) The intensity of the field including the background standing wave that results multiplication of F_F and F_B by the appropriate traveling waves.

The formulation of the FP-LLE in terms of the field ψ defined in the co-moving domain of length $2L$ facilitates numerical simulation of the nonlinear dynamics. To obtain the physical, propagating field in the Fabry-Perot cavity, the arguments of the field ψ are transformed back to dimensionful parameters so that we have $\psi(z,t)$, and then it is boosted to group velocity v_g in the domain of length $2L$ to obtain $\overline{\psi}$, which propagates with periodic boundary conditions $\overline{\psi}(-L,t) = \overline{\psi}(L,t)$. From $\overline{\psi}(z,t)$ we define functions F_F and F_B that are proportional to the forward-propagating and backward-propagating envelopes of the electric field as $F_F(z,t) \propto \overline{\psi}(z,t)$ and $F_B(z,t) \propto \overline{\psi}(-z,t)$, so that they are related by reflection about $z = 0$. The quantity $|F_B(z,t)|^2 + |F_F(z,t)|^2$ on the

physical domain $0 \leq z \leq L$ is then proportional to the intensity in the FP cavity as a function of time, averaged over fast spatial and temporal oscillations associated with the optical frequency. If desired, these can be included by multiplying F_B and F_F by the appropriate traveling waves before summation. This process is depicted schematically in Fig. 1.1.

In the remainder of this chapter we provide an investigation of the nonlinear dynamics in a Fabry-Perot cavity as they relate to the generation of frequency combs. We will focus here exclusively on the properties of FP solitons, as these have been idenfitied as the most promising route towards meeting application needs with Kerr-combs.

1.1 General relationship between the ring LLE and the FP-LLE

As can be seen from Eq. 1.1 for the Fabry-Perot cavity and Eq. **??** for the ring cavity, the difference between the two geometries lies in the term in the FP-LLE $2i\psi \left\langle |\psi|^2 \right\rangle$. This term represents the cross-phase modulation of the field $\psi(\theta, \tau)$ at each co-moving point θ by each other co-moving point θ' as θ and θ' propagate through each other during a round trip of the Fabry Perot cavity. The incorporation of this effect into the FP-LLE as a spatial average is consistent with the inclusion of the drive F and out-coupling $\Delta\omega_{ext}$ (which is included in the damping term $\partial\psi/\partial\tau = -\psi...$) into the LLE as delocalized, constant operators; this approximation is valid for high-finesse cavities, in which the field ψ changes little on the timescale of a round trip.

We can investigate the stationary solutions to the FP-LLE by setting the time derivative to zero, and we find:

$$0 = -(1 + i\alpha)\psi + i|\psi|^2\psi + 2i\psi < |\psi|^2 > -i\frac{\beta_2}{2}\frac{\partial^2\psi}{\partial\theta^2} + F \tag{1.5}$$

$$= -\left(1 + i(\alpha - 2\psi < |\psi|^2 >)\right)\psi + i|\psi|^2\psi - i\frac{\beta_2}{2}\frac{\partial^2\psi}{\partial\theta^2} + F \tag{1.6}$$

$$= -(1 + i\alpha')\psi + i|\psi|^2\psi - i\frac{\beta_2}{2}\frac{\partial^2\psi}{\partial\theta^2} + F, \tag{1.7}$$

where we have defined $\alpha' = \alpha - 2 < |\psi|^2 >$. We can immediately see from Eq. 1.7 that the stationary solutions to the FP-LLE at a point (α, F^2) are the same as the stationary solutions to the ring LLE at the point (α', F^2). Physically, this arises from the need for increased detuning to compensate for the increased Kerr phase-shift due to cross-phase modulation by the full waveform so that the round-trip phase shift is maintained at zero for each point θ in the co-moving frame. As a consequence of this relationship, we expect that the FP-LLE exhibits the same stationary solutions as the ring LLE: Turing patterns and solitons. In the remainder of this chapter we briefly discuss extended patterns (Turing patterns and chaos) in the FP-LLE, and then provide a longer discussion of solitons in the FP-LLE and how they differ from solitons in the ring geometry.

1.2 Extended patterns in the FP-LLE

We confirm the existence of Turing patterns and spatiotemporal chaos under the FP-LLE with numerical simulations of Eq. 1.1. A Turing pattern simulated at the point $(\alpha = 2.5, F^2 = 6)$ is plotted in the θ domain in Fig. 1.2. An interesting contrast between the ring and FP geometries lies in the nature of stationary solutions to Eq. 1.1. For a stationary solution to the ring LLE, the intensity profile remains constant up to simple circulation about the ring at the group velocity. This is not the case for the FP-LLE, where a stationary solution to 1.1 such that $\partial\psi/\partial\tau = 0$ does not correspond to a time-invariant intensity pattern, due to the intensity interference between counter-propagating components of ψ. We demonstrate this by plotting in Fig. 1.2b the physical intensity pattern (averaged over fast spatial and temporal oscillations) in the FP cavity corresponding to the Turing pattern shown in Fig. 1.2a at two different times. As the fields F_F and F_B circulate in the cavity, the number and positions of intensity maxima change.

The FP-LLE also exhibits chaos. In Fig. 1.2c we plot a snapshot of a chaotic waveform simulated at the point $(\alpha = 5.3, F^2 = 8)$. It is interesting to note that as ψ varies in time so

does the average intensity $< |\psi|^2 >$. This leads to a time-varying effective detuning value $\alpha' = \alpha - 2 < |\psi|^2 >$. A natural question, then, is whether this time-varying α' effects the dynamics of chaos. We investigate this by conducting a simulation of chaos with a duration of 10,000 photon lifetimes under the FP-LLE at the point $(\alpha = 5.3, F^2 = 8)$. We then calculate the time-averaged α' value: $\overline{\alpha'} = \alpha - 2\overline{< |\psi|^2 >} = 1.1$, and conduct a ring-LLE simulation at the corresponding point. To compare the dynamics of chaos in each case, we record the amplitudes of local maxima in $|\psi|^2$ throughout the simulation. This data is displayed in histograms in Fig. 1.2d, from which it is apparent that this calculation does not reveal a significant difference between the chaotic dynamics in ring resonator and FP cavities. Nevertheless, this could be an interesting subject to investigate further.

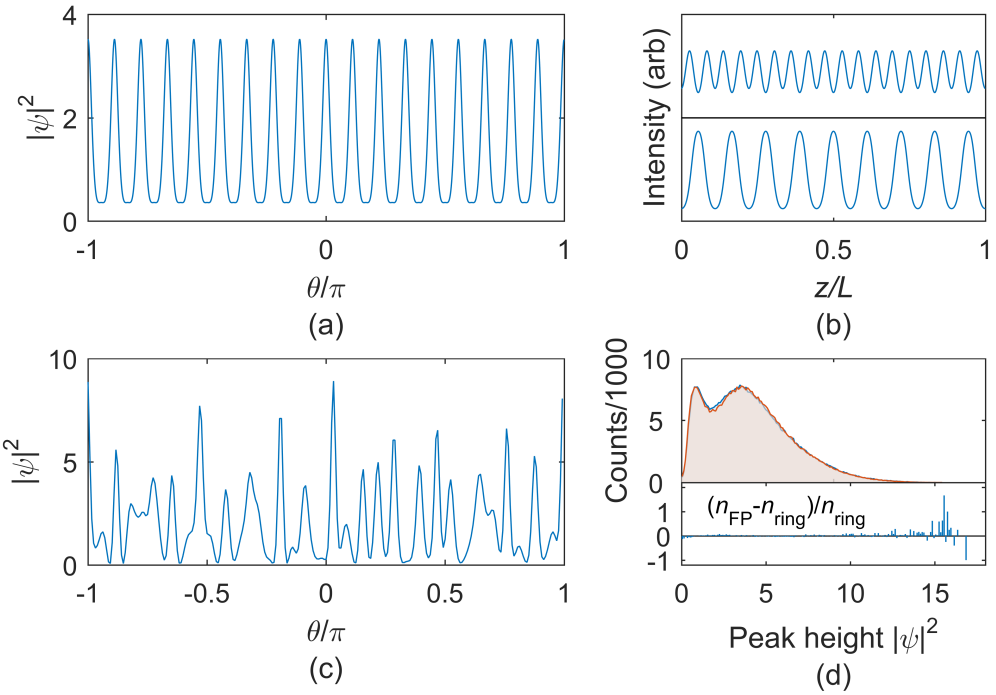

Figure 1.2:

1.3 Solitons in the FP-LLE

1.3.1 Analytical approximation for solitons in the FP-LLE

Equipped with the definition $\alpha' = \alpha - 2 < |\psi|^2 >$ and the relation given in Eq. 1.7, we can investigate the soliton solutions to the FP-LLE. We can immediately adapt the analytical approximation to the soliton solution for the ring LLE, which we recall here for convenience, indicating parameters defined by the detuning for the ring LLE with the 'prime' superscript as in α':

$$\psi_{sol} = \psi'_{s,min} + e^{i\phi'_0}\sqrt{2\alpha'}\,\mathrm{sech}\sqrt{\frac{2\alpha'}{-\beta_2}}\theta. \tag{1.8}$$

Here $\psi'_{s,min}$ is the flat solution to the ring LLE from Eq. **??** at the point where the soliton solution is desired; when multiple flat solutions exist, $\psi'_{s,min}$ is the one corresponding to the smallest intensity ρ'_1 found by solving $F^2 = (1 + (\alpha' - \rho')^2)\rho'$. The phase ϕ'_0 is again defined as $\phi'_0 = \cos^{-1}(\sqrt{8\alpha'}/\pi F)$.

Thus, an approximate soliton solution to the ring LLE according to Eq. 1.8 is also an approximate soliton solution to the FP-LLE at the detuning α, where:

$$\alpha = \alpha' + \frac{1}{\pi}\int d\theta |\psi_{sol}|^2 \tag{1.9}$$

$$= \alpha' + 2\rho_1' + \frac{2}{\pi}\sqrt{-2\alpha'\beta_2}\tanh\left(\pi\sqrt{\frac{2\alpha'}{-\beta_2}}\right) \tag{1.10}$$

$$+ \frac{8}{\pi}\sqrt{-\beta_2\rho_1'}\cos(\phi' - \phi_0')\tan^{-1}\tanh\left(\pi\sqrt{\frac{\alpha'}{-2\beta_2}}\right)$$

and $\phi' = \tan^{-1}(\rho_1' - \alpha')$. To find the approximate soliton solution to the FP-LLE at a point (α, F^2), Eq. 1.10 must be numerically inverted to find α', after which ψ_{sol} can be obtained. As for the ring LLE, an approximation to multi-soliton ensembles is possible as:

$$\psi_{ens} = \psi_{s,min}' + \sqrt{2\alpha'}e^{i\phi_o'}\sum_j \text{sech}\left(\sqrt{\frac{2\alpha'}{-\beta_2}}(\theta - \theta_j)\right). \tag{1.11}$$

Such an ensemble may or may not be stable, depending on the separation between the locations of the solitons $\{\theta_j\}$ and the temporal width of the solitons determined by α' and β_2. Each soliton in the ensemble contributes to the average intensity $< |\psi|^2 >$, so Eq. 1.10 no longer holds; instead, Eq. 1.11 must be integrated to determine a new value for α'.

1.3.2 Existence range of single solitons

An important consequence of the additional nonlinear term $2i\psi\left\langle|\psi|^2\right\rangle$ in the FP-LLE is that the range of parameters over which single solitons exist acquires a dependence on the dispersion parameter β_2, through the effect of dispersion on pulse energy. This is in contrast to the situation for the ring LLE, where the existence range is independent of β_2. For the FP-LLE the existence range also depends on the number of co-propagating pulses and can be greatly extended in the case of many co-propagating solitons; we don't discuss that at length here.

The minimum value of detuning α at which solitons exist as a function of F^2 is determined by the existence of a stable flat solution to the LLE that can form the c.w. background for the soliton. The maximum value of detuning for which solitons can exist is determined by $\alpha' = \alpha - 2\left\langle|\psi|^2\right\rangle$ according to $\alpha'_{max}(F^2) = \pi^2F^2/8$, which approximately gives the maximum detuning for solitons in the ring LLE [53].

For the FP-LLE, a stable flat solution exists to the right of the line $F_+^2(\alpha)$ in the $\alpha - F^2$ plane that bounds from above the region of multiple flat solutions. As we did for the ring LLE, we calculate this line by beginning from the equation describing intensity of the flat stationary solutions ρ to the FP-LLE:

$$F^2 = (1 + (\alpha - 3\rho)^2)\rho. \tag{1.12}$$

There are multiple flat solutions between the values $\rho_\pm$ at which $\partial F^2/\partial\rho = 0$; the upper boundary of this region $F_+^2(\alpha)$ is obtained by inserting $\rho_- = (2\alpha - \sqrt{\alpha^2 - 3})/9)$ into Eq. 1.12:

$$F_+^2(\alpha) = \left[1 + \left(\frac{\alpha + \sqrt{\alpha^2 - 3}}{3}\right)^2\right]\frac{2\alpha - \sqrt{\alpha^2 - 3}}{9} \tag{1.13}$$

This curve bounds the region of soliton existence on the left (lower α) in the limit $\beta_2 \to 0^-$ (β_2 goes to zero from below). In the same limit, the right boundary of soliton existence (higher α) is the line $\alpha_{max}(F^2) = \alpha'_{max}(F^2) + 2\rho_1'(\alpha'_{max}(F^2), F^2)$, where $\rho_1'(\alpha', F^2)$ is the intensity of the smallest flat solution to the ring LLE at (α', F^2).

We can obtain approximations to the bounds of soliton existence for finite β_2 by first finding the amplitudes $\rho_L(F^2)$ and $\rho_R(F^2)$ of the soliton background for the left and right boundaries of soliton existence in the zero-dispersion limit and then using Eq. 1.10 to calculate the value of α at which a soliton exists on a background of that amplitude for finite β_2. These results are summarized in Fig. 1.3. Fig. 1.3a shows the curves corresponding to the $\beta_2 \to 0^-$ limit and for finite β_2 values of -0.001, -0.02, and -0.3, and Fig. 1.3b shows a comparison between the approximate curves for finite β_2 and the soliton existence boundaries as revealed by full simulations of the FP-LLE. The analytical approximation is accurate for low F^2 and small dispersion, but becomes less accurate as these quantities increase. This is because breather solitons whose amplitudes oscillate periodically are found near α_{min} for larger values of F^2. Breather solitons are accompanied by traveling waves that propagate away from the soliton and diminish in amplitude as they do so, and their range increases with the dispersion. For larger values of dispersion these waves fill the cavity, and in this case the flat background whose stability forms the basis for approximating the dispersion-dependent boundary curves is actually not present.

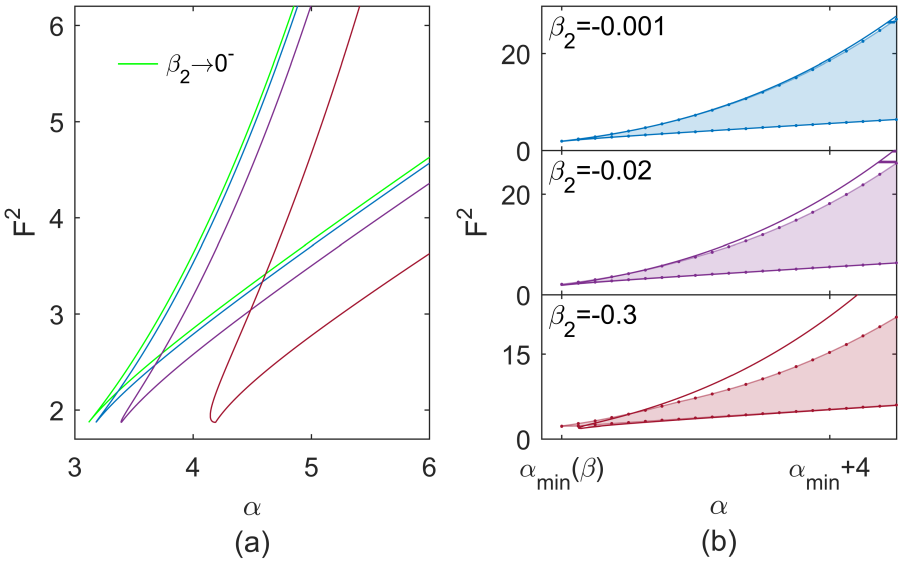

Figure 1.3: **Boundaries of soliton existence in the FP-LLE.** (a) Exact boundary of soliton existence for the limit $\beta_2 \to 0^-$ and analytical approximations to the boundaries for three finite values of dispersion: $\beta_2 = -0.001$ (blue), $\beta_2 = -0.02$ (purple), and $\beta_2 = -.03$ (red). (b) Comparison between the finite-dispersion approximations from (a) and soliton existence boundaries as revealed by full simulations of the FP-LLE.

The lines $\alpha_{min}(F^2)$ and $\alpha_{max}(F^2)$ intersect at $F^2 = F_I^2 \approx 1.87$. Below this value of the pump power solitons do not exist for the FP-LLE, and this can be seen as follows: The value of ρ'_{min} describing the amplitude of the soliton background along the line of maximum detuning α'_{max} for the ring LLE is in general also a flat solution ρ of the FP-LLE at the corresponding point $\alpha_{max} = \alpha'_{max} + 2\rho'_{min}(\alpha'_{max}, F^2)$. However, when $F^2 < F_I^2 \approx 1.87$, the flat solution ρ'_{min} to the ring LLE is not the smallest flat solution to the FP-LLE; instead, it is the middle of three, and is therefore unstable. Therefore, when $F^2 < F_I^2$ the line $\alpha_{max}(F^2)$ as defined above does not represent the right boundary of soliton existence for the FP-LLE. In fact, below this point, for all values of α where a stable flat solution to the FP-LLE ρ_{min} exists, $\alpha - 2\rho_{min}(\alpha, F^2) > \alpha'_{max}$, preventing the existence of solitons. This is an interesting contrast with the ring LLE, where the corresponding lines bounding soliton existence intersect at $F^2 = 1.175$ and where we can verify in simulations that

solitons exist for e.g. $F^2 = 1.5$.

1.3.3 Generation of single solitons through laser frequency scans

A second important consequence of the additional nonlinear term in the FP-LLE relative to the ring LLE is an increase in the range of α values, for a given value of F^2, at which the state of ψ can be either an extended pattern (spatiotemporal chaos or Turing pattern) or a soliton/soliton ensemble. This is because the extended patterns fill the domain and, because of their higher average intensity, experience a greater nonlinear shift than lower duty-cycle single solitons or soliton ensembles due to the additional nonlinear term. Here we discuss the implications of this fact for the experimental generation of single solitons through decreasing-frequency scans of the pump laser, as discussed in Chapter **??**, Sec. **??**. We summarize the results in Fig. 1.4. In Fig. 1.4a we show example simulations of spatiotemporal chaos and a single soliton to illustrate this degeneracy. Both of these simulations are conducted at the point $(\alpha = 8, F^2 = 8)$, and the soliton and chaos are also degenerate with a stable flat solution, with the nature of ψ dependent upon the initial conditions.

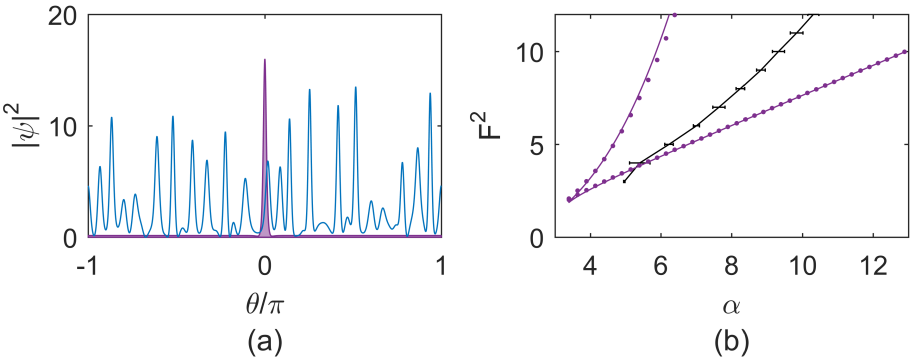

Figure 1.4: **Transition from extended patterns to single solitons in the FP-LLE.** (a) Simulated spatiotemporal chaos (blue) and single soliton solution (purple), either of which can exist at the point $(\alpha = 8, F^2 = 8)$. The amplitude of the soliton is larger than the characteristic amplitude of the features in the chaos because the effective detuning α' is larger for the soliton. (b) Analytical and numerical soliton existence limits (purple) for $\beta = -0.02$ from panel (a) and the upper bound in α for the existence of spatiotemporal chaos/Turing patterns (black with error bars), estimated as described in the text.

It has been established that condensation of solitons from an extended pattern in a sweep in which α increases is a useful way of obtaining single solitons in experiments. Because this method relies on the excitation of an extended pattern (chaos or Turing pattern) to provide initial conditions out of which solitons condense as α is increased, it is important that the maximum detuning (the value of α where $\alpha' = \alpha'_{max} = \pi^2 F^2/8$) for single solitons is larger than the α value at which an extended pattern will transition to a soliton ensemble. Otherwise, the generation of single solitons using this method will be difficult or impossible. To investigate this, we numerically perform slow scans across the resonance to identify where the transition from extended patterns to independent solitons occurs. These scans are conducted slowly to approximate adiabaticity: $d\alpha/d\tau = 2.5 \times 10^{-4}$. We perform 10 scans across the resonance at each integer value of F^2 from 3 to 12 with $\beta = -0.02$, and we identify the transition from extended pattern to independent solitons by inspection of several quantities as α is varied: the set of local maxima and minima of $|\psi|^2$ (see [63]), the distance between local maxima, and the number of local maxima above $|\psi|^2 = 1$. In Fig. 1.4b we plot the line representing the upper boundary in α of extended patterns obtained in the scans across the resonance. Error bars represent the standard deviation of the values α at which the transition is observed, with this spread in the values arising due to the chaotic fluctuations in the total intracavity

power and therefore also in the size of the nonlinear integral term. These results indicate that the region over which single solitons exist and extended patterns do not is narrow for small pump powers F^2, and widens as F^2 is increased. Without performing experiments, it is impossible to precisely quantify the limitations imposed by this observation, but we expect this finding to be useful in refining schemes for single-soliton generation in Fabry-Perot resonators. It is important to note that challenges associated with the necessary transition from high duty-cycle extended patterns to low duty-cycle solitons are alleviated by pulsed pumping, which was the technique used by Obrzud, Lecomte, and Herr in their recent report of soliton generation in FP resonators.

Chapter 2

Microresonator-based frequency combs: Summary and outlook

Chapters **??**-1 discussed generation of frequency combs from a continuous-wave laser by parametric frequecy conversion in Kerr-nonlinear resonators. I described three results: 1. The investigation and implementation of a technique for spontaneous soliton generation in Kerr resonators using a phase-modulated pump laser, 2. The observation and explanation of soliton crystals in Kerr resonators, and 3. A theoretical investigation of Kerr-comb generation in Fabry-Perot cavities, with an emphasis on the properties of solitons and soliton generation. These results all help to more clearly define what is possible with these systems, and suggest avenues for further research.

Soliton generation with a phase-modulated pump laser is a promising candidate for inclusion in chip-integrated Kerr-comb systems as the mechanism by which single-soliton operation is initiated. Two directions for continued work are additional theoretical investigations of the full LLE with a phase-modulated pump, which could provide insight into the dynamics beyond what is possible using the approximations described in Chapter **??**; and implementation of the technique with resonators that have electronically-inaccessible free-spectral ranges, using the subharmonic-modulation approach that was proposed. Incorporation of the technique into a chip-integrated Kerr-soliton comb may also require modification and further devleopment of the technique that was used to overcome thermal instabilities associated with the increasing-frequency pump-laser scan.

The investigation of soliton crystals presented here serves several important purposes. First, it represented an important step towards full explanation of observed Kerr-comb phenomena in terms of the LLE model. Second, soliton crystals have the attractive properties of single-soliton Kerr combs, with the additional property that a soliton crystal of N pulses has conversion efficiency of pump-laser power into the comb that is roughly N times higher than a comparable single-soliton comb. With careful preparation of a particular crystal state, this could make them attractive for applications like optical arbitrary waveform generation and nonlinear spectroscopy. Additionally, soliton crystals present a hugely degenerate configuration space that could be useful in implementations, for example, of an on-chip optical buffer or in communications applications [54]. Finally, experimental generation of soliton crystals is significantly simpler than generation of single solitons, where the change in the duty cycle of the optical waveform from extended pattern to single soliton leads to thermal instabilities that are alleviated only with precise control of the pump-laser power and frequency. Thus, it is possible to propose a scheme for deterministic on-chip soliton crystal generation that makes use of two resonators, each constructed of looped single-mode optical waveguides. One resonator is pumped by a laser and hosts the soliton crystal. The second resonator need not be pumped, and exists to provide a specific perturbation to the mode structure of the first resonator to enable soliton crystallization; this could be achieved through careful engineering of the coupling between the resonators. If the free-spectral range of the second resonator is considerably higher than the free-spectral range of the first, and not near one of its harmonics, then realization of single-mode perturbation to the mode structure of the first resonator could be achieved. Implementing deterministic soliton crystal generation on a chip in this way could greatly simplify requirements on the other components in a system for full-integration of Kerr solitons, as soliton generation could be achieved through slow tuning of the pump laser.

am I citing pascal in sc chapter?

The theoretical investigation of Kerr-comb generation in the Fabry-Perot geometry will pro-

vide useful guidance for future experimental work. An obvious direction for continued work is the generation of solitons in Fabry-Perot cavities that make use of the additional degree of freedom provided by the dispersion applied by reflection at the ends of the cavity. This would build on previous experiments [36, 37]. In fact, soliton generation in Fabry-Perot cavities constructed of potted fiber ferrules with high-reflectivity end-coatings has already been realized at NIST Boulder [**Zhang2018**], but there remains work to be done to achieve control the total cavity dispersion with chirped mirror-coatings. Unresolved questions include the effect of uncontrolled expansion of the mode in the coating on both the mirror reflectivity and its group-velocity disperson. Looking to the chip scale, integrated Fabry-Perot cavities constructued of single-mode waveguides with photonic-crystal mirrors is a promising route for development that would further reduce the footprint of Kerr-comb systems. This work is ongoing at NIST Boulder, and primary comb has been observed in such a cavity [**Yu2018**]. Finally, I note that the proposal for deterministic chip-scale generation of soliton crystals presented above could be realized with two co-linear on-chip Fabry-Perot cavities, where the first cavity hosts the crystal, which is out-coupled in reflection, and the second cavity provides a perturbation to the first cavity's mode structure.

References

[1] Scott A. Diddams, David J. Jones, Jun Ye, Steven T. Cundiff, John L. Hall, Jinendra K. Ranka, Robert S. Windeler, Ronald Holzwarth, Thomas Udem, and T. W. Hänsch. Direct link between microwave and optical frequencies with a 300 THz femtosecond laser comb. *Physical Review Letters*, 84 (22), **2000**, 5102–5105.

[2] David J. Jones, Scott A. Diddams, Jinendra K. Ranka, Andrew Stentz, Robert S. Windeler, John L. Hall, and Steven T. Cundiff. Carrier-Envelope Phase Control of Femtosecond Mode-Locked Lasers and Direct Optical Frequency Synthesis. *Science*, 288 (5466), **2000**, 635–639.

[3] Th Udem, R Holzwarth, and T W Hänsch. Optical frequency metrology. *Nature*, 416 (6877), **2002**, 233–237.

[4] John L. Hall. Nobel lecture: Defining and measuring optical frequencies. *Reviews of Modern Physics*, 78 (4), **2006**, 1279–1295.

[5] Theodor W. Hänsch. Nobel lecture: Passion for precision. *Reviews of Modern Physics*, 78 (4), **2006**, 1297–1309.

[6] Jinendra K. Ranka, Robert S. Windeler, and Andrew J. Stentz. Visible continuum generation in air–silica microstructure optical fibers with anomalous dispersion at 800 nm. *Optics Letters*, 25 (1), **2000**, 25.

[7] S A Diddams, Th Udem, J C Bergquist, E A Curtis, R E Drullinger, L Hollberg, W M Itano, W D Lee, C W Oates, K R Vogel, and D J Wineland. An Optical Clock Based on a Single Trapped 199 Hg+ Ion. *Science (New York, N.Y.)*, 293, **2001**, 825–828.

[8] J. J. McFerran, E. N. Ivanov, A. Bartels, G. Wilpers, C. W. Oates, S. A. Diddams, and L. Hollberg. Low-noise synthesis of microwave signals from an optical source. *Electronics Letters*, 41 (11), **2005**, 650–651. arXiv: `0504102 [arXiv:physics]`.

[9] T. M. Fortier, M. S. Kirchner, F. Quinlan, J. Taylor, J. C. Bergquist, T. Rosenband, N. Lemke, A. Ludlow, Y. Jiang, C. W. Oates, and S. A. Diddams. Generation of ultrastable microwaves via optical frequency division. *Nature Photonics*, 5 (7), **2011**, 425–429. arXiv: `1101.3616`.

[10] Scott A. Diddams, Leo Hollberg, and Vela Mbele. Molecular fingerprinting with the resolved modes of a femtosecond laser frequency comb. *Nature*, 445 (7128), **2007**, 627–630.

[11] Ian Coddington, Nathan Newbury, and William Swann. Dual-comb spectroscopy. *Optica*, 3 (4), **2016**, 414–426.

[12] Steven T. Cundiff and Andrew M. Weiner. Optical arbitrary waveform generation. *Nature Photonics*, 4 (11), **2010**, 760–766.

[13] Tilo Steinmetz, Tobias Wilken, Constanza Araujo-Hauck, Ronald Holzwarth, Theodor W Hänsch, Luca Pasquini, Antonio Manescau, Sandro D'Odorico, Michael T Murphy, Thomas Kentischer, Wolfgang Schmidt, and Thomas Udem. Laser frequency combs for astronomical observations. *Science*, 321 (5894), **2008**, 1335–7.

[14] Brian R. Washburn, Scott A. Diddams, Nathan R. Newbury, Jeffrey W. Nicholson, Man F. Yan, and Carsten G. Jørgensen. Phase-locked, erbium-fiber-laser-based frequency comb in the near infrared. *Optics Letters*, 29 (3), **2004**, 250–252.

[15] Christoph Gohle, Thomas Udem, Maximilian Herrmann, Jens Rauschenberger, Ronald Holzwarth, Hans A. Schuessler, Ferenc Krausz, and Theodor W. Hänsen. A frequency comb in the extreme ultraviolet. *Nature*, 436 (7048), **2005**, 234–237.

[16] Scott A. Diddams. The evolving optical frequency comb [Invited]. *Journal of the Optical Society of America B*, 27 (11), **2010**, B51–B62.

[17] Jerome Faist, Gustavo Villares, Giacomo Scalari, Markus Rosch, Christopher Bonzon, Andreas Hugi, and Mattias Beck. Quantum Cascade Laser Frequency Combs. *Nanophotonics*, 5 (2), **2016**, 272–291. arXiv: 1510.09075.

[18] Daryl T Spencer, Tara Drake, Travis C Briles, Jordan Stone, Laura C Sinclair, Connor Fredrick, Qing Li, Daron Westly, B Robert Ilic, Aaron Bluestone, Nicolas Volet, Tin Komljenovic, Lin Chang, Seung Hoon Lee, Dong Yoon Oh, Tobias J Kippenberg, Erik Norberg, Luke Theogarajan, Myoung-gyun Suh, Ki Youl Yang, H P Martin, Kerry Vahala, Nathan R Newbury, Kartik Srinivasan, John E Bowers, Scott A Diddams, and Scott B Papp. An optical-frequency synthesizer using integrated photonics. *Nature*, 557, **2018**, 81–85.

[19] Travis C. Briles, Jordan R. Stone, Tara E. Drake, Daryl T. Spencer, Connor Frederick, Qing Li, Daron A. Westly, B. Robert Illic, Kartik Srinivasan, Scott A. Diddams, and Scott B. Papp. Kerr-microresonator solitons for accurate carrier-envelope-frequency stabilization. *arXiv*, **2017**, 1711.06251. arXiv: 1711.06251.

[20] Robert W. Boyd. **Nonlinear Optics**. San Diego, CA: Elsevier, 2003.

[21] T M Fortier, David J Jones, and S T Cundiff. Phase stabilization of an octave-spanning Ti:sapphire laser. *Opt. Lett.*, 28 (22), **2003**, 2198–2200.

[22] David R. Carlson, Daniel D. Hickstein, Alex Lind, Stefan Droste, Daron Westly, Nima Nader, Ian Coddington, Nathan R. Newbury, Kartik Srinivasan, Scott A. Diddams, and Scott B. Papp. Self-referenced frequency combs using high-efficiency silicon-nitride waveguides. 42 (12), **2017**, 2314–2317. arXiv: 1704.03909.

[23] David S. Hum and Martin M. Fejer. Quasi-phasematching. *Comptes Rendus Physique*, 8 (2), **2007**, 180–198.

[24] P Del'Haye, A Schliesser, O Arcizet, T Wilken, R Holzwarth, and T J Kippenberg. Optical frequency comb generation from a monolithic microresonator. *Nature*, 450 (7173), **2007**, 1214–1217.

[25] T J Kippenberg, R Holzwarth, and S A Diddams. Microresonator-Based Optical Frequency Combs. *Science (New York, N.Y.)*, 332 (6029), **2011**, 555–559.

[26] A A Savchenkov, A B Matsko, and L Maleki. On Frequency Combs in Monolithic Resonators. *Nanophotonics*, 5, **2016**, 363–391.

[27] Yanne K. Chembo. Kerr optical frequency combs: Theory, applications and perspectives. *Nanophotonics*, 5 (2), **2016**, 214–230.

[28] Alessia Pasquazi, Marco Peccianti, Luca Razzari, David J. Moss, Stéphane Coen, Miro Erkintalo, Yanne K. Chembo, Tobias Hansson, Stefan Wabnitz, Pascal Del'Haye, Xiaoxiao Xue, Andrew M. Weiner, and Roberto Morandotti. Micro-combs: A novel generation of optical sources. *Physics Reports*, 729, **2017**, 1–81.

[29] Hansuek Lee, Tong Chen, Jiang Li, Ki Youl Yang, Seokmin Jeon, Oskar Painter, and Kerry J. Vahala. Chemically etched ultrahigh-Q wedge-resonator on a silicon chip. *Nature Photonics*, 6 (6), **2012**, 369–373. arXiv: 1112.2196.

[30] Xu Yi, Qi-Fan Yang, Ki Youl Yang, Myoung-Gyun Suh, and Kerry Vahala. Soliton frequency comb at microwave rates in a high-Q silica microresonator. *Optica*, 2 (12), **2015**, 1078–1085.

[31] Pascal Del'Haye, Scott A. Diddams, and Scott B. Papp. Laser-machined ultra-high-Q microrod resonators for nonlinear optics. *Applied Physics Letters*, 102, **2013**, 221119.

[32] W Liang, A A Savchenkov, A B Matsko, V S Ilchenko, D Seidel, and L Maleki. Generation of near-infrared frequency combs from a MgF$_2$ whispering gallery mode resonator. *Optics Letters*, 36 (12), **2011**, 2290–2292.

[33] Anatoliy a. Savchenkov, Andrey B. Matsko, Vladimir S. Ilchenko, Iouri Solomatine, David Seidel, and Lute Maleki. Tunable optical frequency comb with a crystalline whispering gallery mode resonator. *Physical Review Letters*, 101 (9), **2008**, 1–4. arXiv: 0804.0263.

[34] Yoshitomo Okawachi, Kasturi Saha, Jacob S. Levy, Y. Henry Wen, Michal Lipson, and Alexander L. Gaeta. Octave-spanning frequency comb generation in a silicon nitride chip. *Optics Letters*, 36 (17), **2011**, 3398–3400. arXiv: 1107.5555.

[35] D J Moss, R Morandotti, A L Gaeta, and M Lipson. New CMOS-compatible platforms based on silicon nitride and Hydex for nonlinear optics. *Nature Photonics*, 7 (July), **2013**, 597–607.

[36] Danielle Braje, Leo Hollberg, and Scott Diddams. Brillouin-Enhanced Hyperparametric Generation of an Optical Frequency Comb in a Monolithic Highly Nonlinear Fiber Cavity Pumped by a cw Laser. *Physical Review Letters*, 102 (19), **2009**, 193902 (cited on pages 1, 10).

[37] Ewelina Obrzud, Steve Lecomte, and Tobias Herr. Temporal solitons in microresonators driven by optical pulses. *Nature Photonics*, 11 (August), **2017**, 600–607. arXiv: 1612.08993 (cited on pages 1, 10).

[38] Vladimir S. Ilchenko and Andrey B. Matsko. Optical resonators with whispering-gallery modes - Part II: Applications. *IEEE Journal on Selected Topics in Quantum Electronics*, 12 (1), **2006**, 15–32.

[39] Ki Youl Yang, Katja Beha, Daniel C. Cole, Xu Yi, Pascal Del'Haye, Hansuek Lee, Jiang Li, Dong Yoon Oh, Scott A. Diddams, Scott B. Papp, and Kerry J. Vahala. Broadband dispersion-engineered microresonator on a chip. *Nature Photonics*, 10 (March), **2016**, 316–320.

[40] Govind P. Agrawal. **Nonlinear Fiber Optics**. 4th. Burlington, MA: Elsevier, 2007.

[41] Maria L Calvo and Vasudevan Lakshminarayanan, eds. **Optical Waveguides: From Theory to Applied Technologies**. Boca Raton, FL: Taylor & Francis, 2007.

[42] A N Oraevsky. Whispering-gallery waves. *Quantum Electronics*, 32 (42), **2002**, 377–400. arXiv: arXiv:1011.1669v3.

[43] Hermann A. Haus. **Waves and Fields in Optoelectronics**. Englewood Cliffs: Prentice-Hall, 1984.

[44] J. C. Knight, G. Cheung, F. Jacques, and T. A. Birks. Phase-matched excitation of whispering-gallery-mode resonances by a fiber taper. *Optics Letters*, 22 (15), **1997**, 1129.

[45] S. M. Spillane, T. J. Kippenberg, O. J. Painter, and K. J. Vahala. Ideality in a Fiber-Taper-Coupled Microresonator System for Application to Cavity Quantum Electrodynamics. *Physical review letters*, 91 (4), **2003**, 043902.

[46] Ehsan Shah Hosseini, Siva Yegnanarayanan, Amir Hossein Atabaki, Mohammad Soltani, and Ali Adibi. Systematic design and fabrication of high-Q single-mode pulley-coupled planar silicon nitride microdisk resonators at visible wavelengths. *Optics Express*, 18 (3), **2010**, 2127.

[47] Tal Carmon, Lan Yang, and Kerry J Vahala. Dynamical thermal behavior and thermal self-stability of microcavities. *Optics Express*, 12 (20), **2004**, 4742–4750.

[48] Raúl del Coso and Javier Solis. Relation between nonlinear refractive index and third-order susceptibility in absorbing media. *Journal of the Optical Society of America B*, 21 (3), **2004**, 640.

[49] T. Kippenberg, S. Spillane, and K. Vahala. Kerr-Nonlinearity Optical Parametric Oscillation in an Ultrahigh-Q Toroid Microcavity. *Physical Review Letters*, 93 (8), **2004**, 083904.

[50] Anatoliy A. Savchenkov, Andrey B. Matsko, Dmitry Strekalov, Makan Mohageg, Vladimir S. Ilchenko, and Lute Maleki. Low threshold optical oscillations in a whispering gallery mode CaF 2 resonator. *Physical Review Letters*, 93 (24), **2004**, 2–5.

[51] Imad H. Agha, Yoshitomo Okawachi, Mark A. Foster, Jay E. Sharping, and Alexander L. Gaeta. Four-wave-mixing parametric oscillations in dispersion-compensated high- Q silica microspheres. *Physical Review A - Atomic, Molecular, and Optical Physics*, 76 (4), **2007**, 1–4.

[52] T. Herr, V. Brasch, J. D. Jost, C. Y. Wang, N. M. Kondratiev, M. L. Gorodetsky, and T. J. Kippenberg. Temporal solitons in optical microresonators. *arXiv*, **2012**, 1211.0733. arXiv: 1211.0733.

[53] T. Herr, V. Brasch, J. D. Jost, C. Y. Wang, N. M. Kondratiev, M. L. Gorodetsky, and T. J. Kippenberg. Temporal solitons in optical microresonators. *Nature Photonics*, 8 (2), **2014**, 145–152. arXiv: 1211.0733 (cited on page 5).

[54] François Leo, Stéphane Coen, Pascal Kockaert, Simon-Pierre Gorza, Philippe Emplit, and Marc Haelterman. Temporal cavity solitons in one-dimensional Kerr media as bits in an all-optical buffer. *Nature Photonics*, 4 (7), **2010**, 471–476 (cited on page 9).

[55] T. Herr, K. Hartinger, J. Riemensberger, C. Y. Wang, E. Gavartin, R. Holzwarth, M. L. Gorodetsky, and T. J. Kippenberg. Universal formation dynamics and noise of Kerr-frequency combs in microresonators. *Nature Photonics*, 6 (7), **2012**, 480–487.

[56] Yanne K. Chembo and Curtis R. Menyuk. Spatiotemporal Lugiato-Lefever formalism for Kerr-comb generation in whispering-gallery-mode resonators. *Physical Review A*, 87, **2013**, 053852.

[57] Stéphane Coen, Hamish G Randle, Thibaut Sylvestre, and Miro Erkintalo. Modeling of octave-spanning Kerr frequency combs using a generalized mean-field Lugiato-Lefever model. *Optics letters*, 38 (1), **2013**, 37–39.

[58] M. Haelterman, S. Trillo, and S. Wabnitz. Dissipative modulation instability in a nonlinear dispersive ring cavity. *Optics Communications*, 91 (5-6), **1992**, 401–407.

[59] T Hansson, M Bernard, and S Wabnitz. Modulational Instability of Nonlinear Polarization Mode Coupling in Microresonators. 35 (4), **2018**. arXiv: arXiv:1802.04535v1.

[60] Y K Chembo, I S Grudinin, and N Yu. Spatiotemporal dynamics of Kerr-Raman optical frequency combs. *Physical Review A*, 92 (4), **2015**, 4.

[61] Cyril Godey, Irina V. Balakireva, Aurélien Coillet, and Yanne K. Chembo. Stability analysis of the spatiotemporal Lugiato-Lefever model for Kerr optical frequency combs in the anomalous and normal dispersion regimes. *Physical Review A*, 89 (6), **2014**, 063814.

[62] I. V. Barashenkov and Yu S. Smirnov. Existence and stability chart for the ac-driven, damped nonlinear Schrödinger solitons. *Physical Review E - Statistical Physics, Plasmas, Fluids, and Related Interdisciplinary Topics*, 54 (5), **1996**, 5707–5725.

[63] A Coillet and Y K Chembo. Routes to spatiotemporal chaos in Kerr optical frequency combs. *Chaos*, 24 (1), **2014**, 5. arXiv: arXiv:1401.0927v1 (cited on page 7).

[64] L A Lugiato and R Lefever. Spatial Dissipative Structures in Passive Optical Systems. *Physical Review Letters*, 58 (21), **1987**, 2209–2211.

[65] LA Lugiato and R Lefever. Diffraction stationary patterns in passive optical systems. *Interaction of Radiation with Matter*, **1987**.

[66] William H. Renninger and Peter T. Rakich. Closed-form solutions and scaling laws for Kerr frequency combs. *Scientific Reports*, 6 (1), **2016**, 24742. arXiv: 1412.4164.

[67] John Scott Russell. Report on Waves. *Fourteenth meeting of the British Association for the Advancement of Science*, **1844**, 311–390.

[68] M. Brambilla, L. A. Lugiato, F. Prati, L. Spinelli, and W. J. Firth. Spatial soliton pixels in semiconductor devices. *Physical Review Letters*, 79 (11), **1997**, 2042–2045.

[69] S. Minardi, F. Eilenberger, Y. V. Kartashov, A. Szameit, U. Röpke, J. Kobelke, K. Schuster, H. Bartelt, S. Nolte, L. Torner, F. Lederer, A. Tünnermann, and T. Pertsch. Three-dimensional light bullets in arrays of waveguides. *Physical Review Letters*, 105 (26), **2010**, 1–4. arXiv: 1101.0734.

[70] F. X. Kärtner, I. D. Jung, and U. Keller. Soliton mode-locking with saturable absorbers. *IEEE Journal on Selected Topics in Quantum Electronics*, 2 (3), **1996**, 540–556.

[71] P. Grelu and N. Akhmediev. Dissipative solitons for mode-locked lasers. *Nature Photonics*, 6 (February), **2012**, 84–92.

[72] L. F. Mollenauer and J. P. Gordon. **Solitons in Optical Fibers**. Academic Press, 2006, p. 296.

[73] A. Hasegawa and Y. Kodama. **Solitons in Optical Communications**. Academic Press, 1995.

[74] Hermann A. Haus and William S. Wong. Solitons in optical communications. *Reviews of Modern Physics*, 68 (2), **1996**, 423–444.

[75] Stéphane Coen and Miro Erkintalo. Universal scaling laws of Kerr frequency combs. *Optics letters*, 38 (11), **2013**, 1790–1792. arXiv: arXiv:1303.7078v1.

[76] H. Guo, M. Karpov, E. Lucas, A. Kordts, M. H.P. Pfeiffer, V. Brasch, G. Lihachev, V. E. Lobanov, M. L. Gorodetsky, and T. J. Kippenberg. Universal dynamics and deterministic switching of dissipative Kerr solitons in optical microresonators. *Nature Physics*, 13 (1), **2017**, 94–102. arXiv: 1601.05036.

[77] N. J. Zabusky and M. D. Kruskal. Interaction of "solitons" in a collisionless plasma and the recurrence of initial states. *Physical Review Letters*, 15 (6), **1965**, 240.

[78] J P Gordon. Interaction forces among solitons in optical fibers. *Optics Letters*, 8 (11), **1983**, 596.

[79] Boris A. Malomed. Bound solitons in the nonlinear Schrodinger-Ginzburg-Landau equation. *Physical Review A*, 44 (10), **1991**, 6954–6957.

[80] J K Jang, M Erkintalo, S G Murdoch, and S Coen. Ultraweak long-range interactions of solitons observed over astronomical distances. *Nature Photonics*, 7 (8), **2013**, 657–663. arXiv: arXiv:1305.6670v1.

[81] Pedro Parra-Rivas, Damia Gomila, Pere Colet, and Lendert Gelens. Interaction of solitons and the formation of bound states in the generalized Lugiato-Lefever equation. *European Physical Journal D*, 71 (7), **2017**, 198. arXiv: arXiv:1705.02619v1.

[82] Yadong Wang, François Leo, Julien Fatome, Miro Erkintalo, Stuart G. Murdoch, and Stéphane Coen. Universal mechanism for the binding of temporal cavity solitons, **2017**, 1–10. arXiv: 1703.10604.

[83] Victor Brasch, Tobias Herr, Michael Geiselmann, Grigoriy Lihachev, Martin H. P. Pfeiffer, Michael L. Gorodetsky, and Tobias J. Kippenberg. Photonic chip-based optical frequency comb using soliton Cherenkov radiation. *Science*, 351 (6271), **2016**, 357. arXiv: 1410.8598 (cited on page 1).

[84] Jordan R Stone, Travis C Briles, Tara E Drake, Daryl T Spencer, David R Carlson, Scott A Diddams, and Scott B Papp. Thermal and Nonlinear Dissipative-Soliton Dynamics in Kerr Microresonator Frequency Combs. *arXiv*, **2017**, 1708.08405. arXiv: 1708.08405.

[85] V. E. Lobanov, G. V. Lihachev, N. G. Pavlov, A. V. Cherenkov, T. J. Kippenberg, and M. L. Gorodetsky. Harmonization of chaos into a soliton in Kerr frequency combs. *Optics Express*, 24 (24), **2016**, 27382. arXiv: 1607.08222.

[86] Chaitanya Joshi, Jae K. Jang, Kevin Luke, Xingchen Ji, Steven A. Miller, Alexander Klenner, Yoshitomo Okawachi, Michal Lipson, and Alexander L. Gaeta. Thermally controlled comb generation and soliton modelocking in microresonators. *Optics Letters*, 41 (11), **2016**, 2565–2568. arXiv: 1603.08017.

[87] Weiqiang Wang, Zhizhou Lu, Wenfu Zhang, Sai T. Chu, Brent E. Little, Leiran Wang, Xiaoping Xie, Mulong Liu, Qinghua Yang, Lei Wang, Jianguo Zhao, Guoxi Wang, Qibing Sun, Yuanshan Liu, Yishan Wang, and Wei Zhao. Robust soliton crystals in a thermally controlled microresonator. *Optics Letters*, 43 (9), **2018**, 2002–2005.

[88] Jae K Jang, Miro Erkintalo, Stuart G Murdoch, and Stéphane Coen. Writing and erasing of temporal cavity solitons by direct phase modulation of the cavity driving field. *Optics Letters*, 40 (20), **2015**, 4755–4758. arXiv: 1501.05289.

[89] Jae K Jang, Miro Erkintalo, Stephane Coen, and Stuart G Murdoch. Temporal tweezing of light through the trapping and manipulation of temporal cavity solitons. *Nature Communications*, 6, **2015**, 7370. arXiv: 1410.4836.

[90] Yadong Wang, Bruno Garbin, Francois Leo, Stephane Coen, Miro Erkintalo, and Stuart G. Murdoch. Writing and Erasure of Temporal Cavity Solitons via Intensity Modulation of the Cavity Driving Field. *arXiv*, **2018**, 1802.07428. arXiv: 1802.07428.

[91] Scott B. Papp, Katja Beha, Pascal Del'Haye, Franklyn Quinlan, Hansuek Lee, Kerry J. Vahala, and Scott A. Diddams. Microresonator frequency comb optical clock. *Optica*, 1 (1), **2014**, 10–14. arXiv: 1309.3525.

[92] Myoung Gyun Suh, Qi Fan Yang, Ki Youl Yang, Xu Yi, and Kerry J. Vahala. Microresonator soliton dual-comb spectroscopy. *Science*, 354 (6312), **2016**, 1–5. arXiv: 1607.08222.

[93] Pablo Marin-Palomo, Juned N. Kemal, Maxim Karpov, Arne Kordts, Joerg Pfeifle, Martin H.P. Pfeiffer, Philipp Trocha, Stefan Wolf, Victor Brasch, Miles H. Anderson, Ralf Rosenberger, Kovendhan Vijayan, Wolfgang Freude, Tobias J. Kippenberg, and Christian Koos. Microresonator-based solitons for massively parallel coherent optical communications. *Nature*, 546 (7657), **2017**, 274–279. arXiv: 1610.01484.

[94] J. D. Jost, T. Herr, C. Lecaplain, V. Brasch, M. H. P. Pfeiffer, and T. J. Kippenberg. Counting the cycles of light using a self-referenced optical microresonator. *Optica*, 2 (8), **2015**, 706–711. arXiv: 1411.1354.

[95] Pascal Del'Haye, Aurélien Coillet, Tara Fortier, Katja Beha, Daniel C. Cole, Ki Youl Yang, Hansuek Lee, Kerry J. Vahala, Scott B. Papp, and Scott A. Diddams. Phase-coherent microwave-to-optical link with a self-referenced microcomb. *Nature Photonics*, 10 (June), **2016**, 1–5.

[96] Victor Brasch, Erwan Lucas, John D. Jost, Michael Geiselmann, and Tobias J. Kippenberg. Self-referenced photonic chip soliton Kerr frequency comb. *Light: Science & Applications*, 6 (1), **2017**, e16202. arXiv: 1605.02801.

[97] Hossein Taheri, Ali A. Eftekhar, Kurt Wiesenfeld, and Ali Adibi. Soliton formation in whispering-gallery-mode resonators via input phase modulation. *IEEE Photonics Journal*, 7 (2), **2015**, 2200309.

[98] M. Zajnulina, M. Böhm, D. Bodenmüller, K. Blow, J.M. Chavez Boggio, A.A. Rieznik, and M.M. Roth. Characteristics and stability of soliton crystals in optical fibres for the purpose of optical frequency comb generation. *Optics Communications*, 393 (November 2016), **2017**, 95–102.

[99] Adil Haboucha, Hervé Leblond, Mohamed Salhi, Andrey Komarov, and François Sanchez. Coherent soliton pattern formation in a fiber laser. *Optics Letters*, 33 (5), **2008**, 524–526.

[100] Foued Amrani, Mohamed Salhi, Philippe Grelu, Hervé Leblond, and François Sanchez. Universal soliton pattern formations in passively mode-locked fiber lasers. *Optics letters*, 36 (9), **2011**, 1545–1547.

[101] A. Haboucha, H. Leblond, M. Salhi, A. Komarov, and F. Sanchez. Analysis of soliton pattern formation in passively mode-locked fiber lasers. *Physical Review A*, 78, **2008**, 043806.

[102] B A Malomed, A Schwache, and F Mitschke. Soliton lattice and gas in passive fiber-ring resonators. *Fiber and Integrated Optics*, 17 (4), **1998**, 267–277.

[103] F. Mitschke and A. Schwache. Soliton ensembles in a nonlinear resonator. *Journal of Optics B: Quantum and Semiclassical Optics*, 10 (6), **1998**, 779–788.

[104] A. Schwache and F. Mitschke. Properties of an optical soliton gas. *Physical Review E*, 55 (6), **1997**, 7720–7725.

[105] Hermann A. Haus and Weiping Huang. Coupled-Mode Theory. *Proceedings of the IEEE*, 79 (10), **1991**, 1505–1518.

[106] A A Savchenkov, A B Matsko, W Liang, V S Ilchenko, D Seidel, and L Maleki. Kerr frequency comb generation in overmoded resonators. *Opt Express*, 20 (24), **2012**, 27290–27298. arXiv: `arXiv:1201.1959v1`.

[107] T. Herr, V. Brasch, J. D. Jost, I. Mirgorodskiy, G. Lihachev, M. L. Gorodetsky, and T. J. Kippenberg. Mode Spectrum and Temporal Soliton Formation in Optical Microresonators. *Physical Review Letters*, 113 (12), **2014**, 123901.

[108] Yang Liu, Yi Xuan, Xiaoxiao Xue, Pei-Hsun Wang, Steven Chen, Andrew J. Metcalf, Jian Wang, Daniel E. Leaird, Minghao Qi, and Andrew M. Weiner. Investigation of mode coupling in normal-dispersion silicon nitride microresonators for Kerr frequency comb generation. *Optica*, 1 (3), **2014**, 137–144.

[109] Xiaoxiao Xue, Yi Xuan, Yang Liu, Pei-Hsun Wang, Steven Chen, Jian Wang, Dan E Leaird, Minghao Qi, and Andrew M Weiner. Mode-locked dark pulse Kerr combs in normal-dispersion microresonators. *Nat Photon*, 9 (9), **2015**, 594–600.

[110] Chengying Bao, Yi Xuan, Daniel E. Leaird, Stefan Wabnitz, Minghao Qi, and Andrew M. Weiner. Spatial mode-interaction induced single soliton generation in microresonators. *Optica*, 4 (9), **2017**, 1011.

[111] T. Hansson and S. Wabnitz. Bichromatically pumped microresonator frequency combs. *Physical Review A*, 90, **2014**, 013811. arXiv: `1404.2792`.

[112] D V Skryabin and William J. Firth. Interaction of cavity solitons in degenerate optical parametric oscillators. *Optics letters*, 24 (15), **1999**, 1056–1058. arXiv: `9906004 [patt-sol]`.

[113] S. Wabnitz. Control of soliton train transmission, storage, and clock recovery by cw light injection. *Journal of the Optical Society of America B*, 13 (12), **1996**, 2739–2749.

[114] J. A. Barker and D. Henderson. What is "liquid"? Understanding the states of matter. *Reviews of Modern Physics*, 48 (4), **1976**, 587–671.

[115] Takeshi Egami and Simon Billinge. **Underneath the Bragg Peaks**. 2nd. Oxford, UK: Elsevier, 2012, p. 422.

[116] Niel W. Ashcroft and David N. Mermin. **Solid State Physics**. 1st ed. Belmont, CA: Brooks/Cole, 1976, p. 826.

[117] Andrew Weiner. **Ultrafast Optics**. 1st ed. Hoboken, NJ: Wiley, 2009, p. 598.

[118] T. Kobayashi, T. Sueta, Y. Cho, and Y. Matsuo. High-repetition-rate optical pulse generator using a Fabry-Perot electro-optic modulator. *Applied Physics Letters*, 21 (8), **1972**, 341–343.

[119] Motonobu Kourogi, Ken Nakagawa, and Motoichi Ohtsu. Wide-Span Optical Frequency Comb Generator for. 29 (10), **1993**.

[120] H. Murata, A. Morimoto, T. Kobayashi, and S. Yamamoto. Optical pulse generation by electrooptic-modulation method and its application to integrated ultrashort pulse generators. *IEEE Journal of Selected Topics in Quantum Electronics*, 6 (6), **2000**, 1325–1331.

[121] Takahide Sakamoto, Tetsuya Kawanishi, and Masayuki Izutsu. Asymptotic formalism for ultraflat optical frequency comb generation using a Mach-Zehnder modulator. *Optics letters*, 32 (11), **2007**, 1515–1517.

[122] Isao Morohashi, Takahide Sakamoto, Hideyuki Sotobayashi, Tetsuya Kawanishi, Iwao Hosako, and Masahiro Tsuchiya. Widely repetition-tunable 200 fs pulse source using a Mach-Zehnder-modulator-based flat comb generator and dispersion-flattened dispersion-decreasing fiber. *Optics letters*, 33 (11), **2008**, 1192–1194.

[123] A. Ishizawa, T. Nishikawa, A. Mizutori, H. Takara, S. Aozasa, A. Mori, H. Nakano, A. Takada, and M. Koga. Octave-spanning frequency comb generated by 250 fs pulse train emitted from 25 GHz externally phase-modulated laser diode for carrier-envelope-offset-locking. *Electronics Letters*, 46 (19), **2010**, 1343.

[124] Rui Wu, V. R. Supradeepa, Christopher M. Long, Daniel E. Leaird, and Andrew M. Weiner. Generation of very flat optical frequency combs from continuous-wave lasers using cascaded intensity and phase modulators driven by tailored radio frequency waveforms. *Optics Letters*, 35 (19), **2010**, 3234. arXiv: `1005.5373`.

[125] V. R. Supradeepa and Andrew M. Weiner. Bandwidth scaling and spectral flatness enhancement of optical frequency combs from phase-modulated continuous-wave lasers using cascaded four-wave mixing. *Optics Letters*, 37 (15), **2012**, 3066.

[126] Andrew J Metcalf, Victor Torres-company, Daniel E Leaird, Senior Member, Andrew M Weiner, and Abstract Broadband. High-Power Broadly Tunable Electrooptic Frequency Comb Generator. *IEEE Journal of Selected Topics in Quantum Electronics*, 19 (6), **2013**, 3500306.

[127] Rui Wu, Victor Torres-company, Daniel E Leaird, and Andrew M Weiner. Optical Frequency Comb Generation. 21 (5), **2013**, 6045–6052.

[128] John M. Dudley, Goëry Goery Genty, and Stéphane Coen. Supercontinuum generation in photonic crystal fiber. *Reviews of Modern Physics*, 78 (4), **2006**, 1135–1184.

[129] A. M. Weiner. Femtosecond pulse shaping using spatial light modulators. *Review of Scientific Instruments*, 71 (5), **2000**, 1929–1960.

[130] a a Amorim, M V Tognetti, P Oliveira, J L Silva, L M Bernardo, F X Kärtner, and H M Crespo. Sub-two-cycle pulses by soliton self-compression in highly nonlinear photonic crystal fibers. *Optics letters*, 34 (24), **2009**, 3851–3853.

[131] Gianni Di Domenico, Stéphane Schilt, and Pierre Thomann. Simple approach to the relation between laser frequency noise and laser line shape. *Applied optics*, 49 (25), **2010**, 4801–4807.

[132] William C. Swann, Esther Baumann, Fabrizio R. Giorgetta, and Nathan R. Newbury. Microwave generation with low residual phase noise from a femtosecond fiber laser with an intracavity electro-optic modulator. *Optics Express*, 19 (24), **2011**, 24387. arXiv: `arXiv:1106.5195v1`.

[133] Jiang Li, Xu Yi, Hansuek Lee, Scott A Diddams, and Kerry J Vahala. Electro-optical frequency division and stable microwave synthesis. *Science*, 345 (6194), **2014**, 309–314.

[134] Judah Levine. Introduction to time and frequency metrology. *Review of Scientific Instruments*, 70 (6), **1999**, 2567–2596.

[135] David R. Carlson, Daniel D. Hickstein, Daniel C. Cole, Scott A. Diddams, and Scott B. Papp. Dual-comb interferometry via repetition-rate switching of a single frequency comb. *arXiv*, **2018**, 1806.05311. arXiv: `1806.05311`.

[136] A. J. Metcalf, C. Bender, S. Blakeslee, W. Brand, D. Carlson, S. A. Diddams, C. Fredrick, S. Halverson, F. Hearty, D. Hickstein, J. Jennings, S. Kanodia, K. Kaplan, E. Lubar, S. Mahadevan, A. Monson, J. Ninan, C. Nitroy, S. Papp, L. Ramsey, P. Robertson, A. Roy, C. Schwab, K. Srinivasan, G. K. Stefansson, and R. Terrien. Infrared Astronomical Spectroscopy for Radial Velocity Measurements with 10 cm/s Precision. In: **Conference on Lasers and Electro-Optics**. 2018, JTh5A.1.

[137] Sterling Backus, Charles G. Durfee, Margaret M. Murnane, and Henry C. Kapteyn. High power ultrafast lasers. *Review of Scientific Instruments*, 69 (3), **1998**, 1207.

[138] Andrius Baltuska, Matthias Uiberacker, Eleftherios Goulielmakis, Reinhard Kienberger, Vladislav S Yakovlev, Thomas Udem, Theodor W Hänsch, and Ferenc Krausz. Phase-Controlled Amplification of Few-Cycle Laser Pulses. *IEEE Journal of Selected Topics in Quantum Electronics*, 9 (4), **2003**, 972–989.

[139] Christoph Gohle, Jens Rauschenberger, Takao Fuji, Thomas Udem, Alexander Apolonski, Ferenc Krausz, and Theodor W Hänsch. Carrier envelope phase noise in stabilized amplifier systems. 30 (18), **2005**, 2487–2489.

[140] J. Rauschenberger, T. Fuji, M. Hentschel, A.-J. Verhoef, T. Udem, C. Gohle, T. W. Hänsch, and F. Krausz. Carrier-envelope phase-stabilized amplifier system. *Laser Physics Letters*, 3 (1), **2006**, 37–42.

[141] M E Fermann, V I Kruglov, B C Thomsen, J M Dudley, and J D Harvey. Self-similar propagation and amplification of parabolic pulses in optical fibers. *Physical review letters*, 84 (26 Pt 1), **2000**, 6010–3.

[142] Masaaki Hirano, Tetsuya Nakanishi, Toshiaki Okuno, and Masashi Onishi. Silica-Based Highly Nonlinear Fibers and Their Application. *Sel. Top. Quantum Electron.*, 15 (1), **2009**, 103–113.

[143] Dimitrios Mandridis, Ibrahim Ozdur, Franklyn Quinlan, Mehmetcan Akbulut, Jason J Plant, Paul W Juodawlkis, and Peter J Delfyett. Low-noise, low repetition rate, semiconductor-based mode-locked laser source suitable for high bandwidth photonic analog – digital conversion. *Applied Optics*, 49 (15), **2010**, 2850–2857.

[144] Hans-A. Bachor and Peter J. Manson. Practical Implications of Quantum Noise. *Journal of Modern Optics*, 37 (11), **1990**, 1727–1740.

[145] Franklyn Quinlan, Tara M. Fortier, Haifeng Jiang, and Scott a. Diddams. Analysis of shot noise in the detection of ultrashort optical pulse trains. *Journal of the Optical Society of America B*, 30 (6), **2013**, 1775.

[146] Daniel C. Cole, Katja M. Beha, Scott A. Diddams, and Scott B. Papp. Octave-spanning supercontinuum generation via microwave frequency multiplication. *Proceedings of the 8th Sympsion on Frequency Standards and Metrology 2015, Journal of Physics: Conference Series*, 723, **2016**, 012035.

[147] Alexander M Heidt. Efficient Adaptive Step Size Method for the Simulation of Supercontinuum Generation in Optical Fibers. *Journal of Lightwave Technology*, 27 (18), **2009**, 3984–3991.

[148] J. Hult. A Fourth-Order Runge-Kutta in the Interaction Picture Method for Simulating Supercontinuum Generation in Optical Fibers. *Journal of Lightwave Technology*, 25 (12), **2007**, 3770–3775.

[149] Katja Beha, Daniel C. Cole, Pascal Del'Haye, Aurélien Coillet, Scott A. Diddams, and Scott B. Papp. Electronic synthesis of light. *Optica*, 4 (4), **2017**, 406–411.

[150] Rachid Driad, Josef Rosenzweig, Robert Elvis Makon, Rainer Lösch, Volker Hurm, Herbert Walcher, and Michael Schlechtweg. InP DHBT-Based IC Technology for 100-Gb / s Ethernet. *IEEE Trans. on Electron. Devices*, 58 (8), **2011**, 2604–2609.

[151] Damir Ferenci, Markus Grozing, Manfred Berroth, Robert Makon, Rachid Driad, and Josef Rosenzweig. A 25 GHz Analog Demultiplexer with a Novel Track and Hold Circuit for a 50 GS / s A / D-Conversion System in InP DHBT Technology. In: **Microwave Symposium Digest**. 2012, pp. 1–3.

[152] Kensuke Ikeda. Multiple-valued stationary state and its instability of the transmitted light by a ring cavity system. *Optics Communications*, 30 (2), **1979**, 257–261.

[153] K J Blow and D Wood. Theoretical description of transient stimulated Raman scattering in optical fibers. *Quantum Electronics, IEEE Journal of*, 25 (12), **1989**, 2665–2673.